

## NANO-DIMENSIONAL MEASUREMENT USING OPTICALLY TRAPPED PROBE ENHANCED BY INTERFEROMETRIC SCALE

*Masaki Michihata, Daisuke Nakai, Terutake Hayashi and Yasuhiro Takaya*

Osaka University, Department of Mechanical Engineering, Suita, Japan,  
michihata@optim.mech.eng.osaka-u.ac.jp

**Abstract** – We propose a new dimensional measurement technique that is capable of measuring the bottom surface of a stepwise shape. The measurement system is composed of a length scale and a sensor probe to read the scale. The probe is trapped and controlled three-dimensionally by laser trapping technique. The scale is arisen by optical interference, which is extended straight to the measured surface from the probe. Firstly measurement principle is theoretically explained. Remarkable feature of this technique is feasibility to access the area as narrow as  $15\ \mu\text{m}$ . Vertical resolution of this measurement technique is experimentally estimated as  $10\ \text{nm}$ . The measurable range of the inclination angle of surface is less than  $15^\circ$ . In terms of the measurement accuracy, it is evaluated around  $100\ \text{nm}$ .

**Keywords:** Standing wave, Laser trap, Interference scale

### 1. INTRODUCTION

Accelerated complexity of miniature products requires precisely manufactured micro-components such as micro-lens and micro-gears. Therefore, the measurement technology for inspecting 3-dimensional shapes of micro-components is highly demanded. Then, various instruments [1,2] such as the profilometer [3], the optical microscopes [4], the electron microscopy, the scanning probe microscopy and the coordinate measuring machine [5] have been developed so far. However, it is still difficult to measure the stepwise shape appeared in the grooves and fresnel lens etc., because a probe can hardly access the bottom surface. Then, we propose a new dimensional measurement technique that is capable of measuring the bottom surface of a stepwise object.

The measurement system proposed is composed of a length scale and a sensor probe to read the scale. The probe is trapped and controlled three dimensionally by laser trapping technique [6]. The scale is arisen by optical interference, which is extended straight to measured surface from the probe. Typically a length of the scale is  $100\ \mu\text{m}$  or more and the scale is as thin as a few dozen  $\mu\text{m}$  in diameter. So, an aspect ratio is around 10. Using the scale, a distance between the probe and the surface is measured by a sensor probe. Dimension of an object is measured by scanning over the object. The remarkable properties of this technique are as follows.

- It is accessible to narrow area.
- Working distance to the surface is wide.
- Measured dimension is assured by laser wavelength.

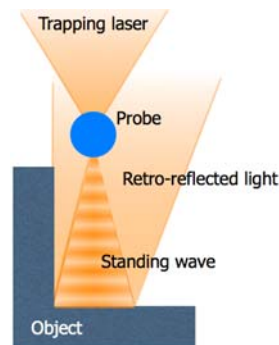


Fig.1. Concept of technique.

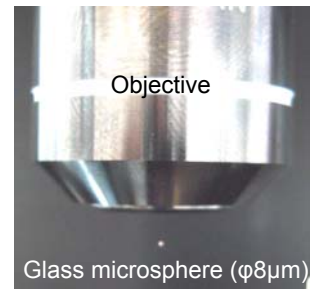


Fig.2. Optically trapped probe.

In this paper, as a fundamental study, this measurement principle is theoretically confirmed and the measurement properties such as the measurable range, the accuracy and the resolution are experimentally investigated. Finally, a feasibility of dimensional measurement by using this technique is examined.

### 2. PRINCIPLE OF MEASUREMENT

The proposed measurement concept is illustrated in Figure 1, which integrates an interference pattern and an optically trapped micro-probe. A glass microsphere is optically trapped in air by a focused laser (trapping laser) as shown in Figure 2. Steep gradient of optical potential generated by the focused laser confines the microsphere nearby the laser focus. This optically trapped micro-sphere acts as a probe to read the scales. The trapping laser beyond the micro-sphere reaches the surface to be measured. When a measured laid on the optical axis shown in Figure 1, a retro-reflected light and the trapping laser generate a standing wave pattern along with the optical axis [7]. A pitch of the standing wave pattern is subjected to the trapping laser wavelength. Thereby, the standing wave performs as the fiduciary length scale, which is named as an interferometric scale. Since an interferometric scale origin is rooted on the measured surface, the probe measures the surface displacement along the optical axis by counting the divisions of the scale. The point is that the light illuminated area on the surface is small due to the lens effect by the trapped microsphere, therefore, the sensor probe detects only paraxial standing wave. As the result, this technique makes it possible to access the narrow area on the bottom surface of the stepwise shape.

The probe originally stays at the stable position. Once the probe is in standing wave pattern, the forces act on the probe in a spatially periodic potential formed by the interferometric scale, which positionally-modulates the probe within optical trapping potential. When the probe crosses over one pitch of the standing wave pattern, the probe returns to the original position. Figure 3 depicts the image of reading the scale. In this manner, displacement of the measured surface is converted into probe repetitive motion. Thus, distance between a measured surface and the probe center is measured by monitoring probe motion. A probe locates a position where the forces by the trapping laser and the interferometric scale equilibrate. To understand the probe behavior, a optical trapping force and a force by standing wave potential are theoretically analyzed.

### 3. THEORETICAL ANALYSIS

#### 3.1 Optical trapping force

A. Ashkin first demonstrates single beam gradient-force trapping for a dielectric particle in 1986 [6] and analyzed trapping forces in ray optics regime by means of a ray-trace method in 1992 [8]. As shown, for a large sphere compared with a wavelength of the trapping laser, trapping forces derived from optical radiation pressure can be analyzed by ray trace method.

Figure 4 illustrates the simulation model for the axial trapping forces. The laser beam having radius,  $r_{max}$ , is focused by an objective lens with high numerical aperture (NA). Then, maximum incident angle  $\phi_{max}$  is calculated by using the relation of  $\phi_{max} = \sin^{-1}(NA(n_1/n_2))$ . In case of NA0.95,  $\phi_{max}$  is 72°. Incident beam is divided into the numbers of optical rays. The total trapping force is sum of the force component generated by all rays. And the trapping force itself is composed of scattering and gradient forces, which are forces that directs in parallel and perpendicular to the direction of an optical ray, respectively. The scattering and gradient forces are calculated by using the equations as follows [8]:

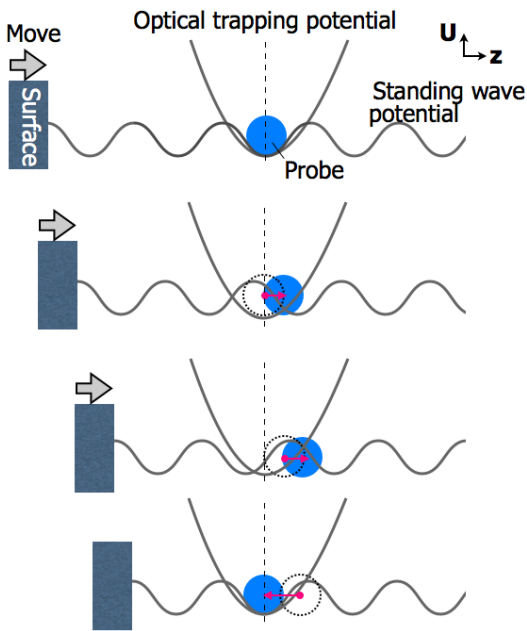


Fig.3. Schematic image of positional deviation of the probe.

$$F_s = \frac{n_1 P}{c} \left\{ 1 + R \cos 2\theta_i - \frac{T^2 \{ \cos 2(\theta_i - \theta_r) + R \cos 2\theta_i \}}{1 + R^2 + 2R \cos 2\theta_r} \right\} \quad (1)$$

$$F_g = \frac{n_1 P}{c} \left\{ R \sin 2\theta_i - \frac{T^2 \{ \sin 2(\theta_i - \theta_r) + R \sin 2\theta_i \}}{1 + R^2 + 2R \cos 2\theta_r} \right\} \quad (2)$$

Contributions in axial direction of these forces are  $-F_s \cos \phi_i$ ,  $F_g \sin \phi_i$ , respectively, so that the axial force of each ray is  $F_{zi} = -F_s \cos \phi_i + F_g \sin \phi_i$ . To obtain the total axial force component for the whole laser beam,  $F_{zi}$  is integrated as following equation.

$$F_z = \int_0^{2\pi} \int_0^{r_{max}} F_{zi} dr d\beta \quad (3)$$

where,  $\beta$  is the azimuthal angle around the optical axis.

In this system, the probe is deviated axially from the laser focus. The axially deviated distance is indicated as  $d_z$ . Figure 5 shows the computed axial trapping force components. The circle represents the probe. Mass of the probe is comparably small (appro. 5 pN) so that, it is negligible. From the simulation result, it is shown that the probe is always trapped around 1  $\mu\text{m}$  below the laser focus. The trapping force exerted to the probe is linear at  $d_z$  from 3  $\mu\text{m}$  to -2  $\mu\text{m}$ . In this range, the axial trapping force is regarded as a simple spring force such as follows:

$$F_r = -kx_r \quad (4)$$

where,  $k$  is the vertical spring constant induced from the axial trapping force,  $d_r$  is the distance between the laser focus and the center of the probe.  $k$  depends on the probe diameter, laser power, material of the probe etc. Thus, by using numerical analysis,  $k$  is estimated as 26  $\mu\text{N/m}$  for a glass particle of 8  $\mu\text{m}$  in diameter and an irradiated laser power of 100 mW.

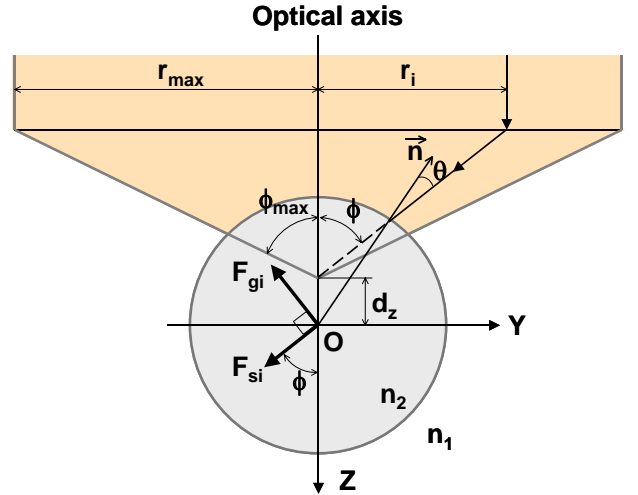


Fig. 4. Geometrical model of computer simulation for analyzing the axial trapping force in single-laser gradient-force trap. The symbols represent the units as follows.  $r_{max}$  is a radius of the laser beam,  $r_i$ , radial distance of a ray,  $n$ , normal vector of the surface where a ray strikes,  $d_z$ , distance between the axially deviated laser focus and the center of the probe,  $\phi_{max}$ , maximum focusing angle for optical axis,  $\phi$ , focusing angle,  $\theta$ , incident angle at a probe surface,  $n_1$ , refractive index of surrounding media,  $n_2$ , refractive index of a probe,  $F_{gi}$ ,  $F_{si}$ , gradient force and scattering force generated by a ray, respectively.

### 3.2 Forces by standing wave potential

In a single laser gradient force trapping, the trapping laser propagates beyond the probe as forward-scattering light. Interference of this forward-scattering light and retro-reflected light from the measured surface generates a standing wave surrounding the probe. The standing wave induces the external force for the probe [9]. Due to gaussian intensity profile of the laser source, the paraxial beam mainly generates forces. Supposed that the incident beam,  $E_i$  and the reflected beam,  $E_r$ , electric fields have the forms of

$$E_i = E_1 \cos(kz + \varepsilon) \quad (5)$$

$$E_r = E_2 \cos(-kz + \pi + \varepsilon) \quad (6)$$

where  $E_1$  and  $E_2$  is the amplitude,  $k$  is the wave number and  $\varepsilon$  is the initial phase. By considering a superimposition of  $E_i$  and  $E_r$ , the intensity of the standing wave along optical axis is described as follows:

$$I(z) = I_o [1 + \alpha \cos(4\pi z / \lambda)] \quad (7)$$

where,  $I_o$  is the average intensity and  $\lambda$  is the wavelength of the trapping laser,  $z$  is the distance of the laser focus from the measured surface, and  $\alpha$  is a value regarding to the reflective property of the measured surface. From the equation, the pitch of the standing wave is  $\lambda/2$ . In this standing wave, the probe experiences the axial external force,  $F_s$  [9]

$$F_s = A \sin(4\pi z / \lambda) \quad (8)$$

where  $A$  is amplitude of the standing wave depending mainly on the reflective index of the measured surface and the laser power.

### 3.3 Probe position

Axial position of the probe between the trapping laser and measured surface is controlled by the forces by the trapping laser  $F_r$ , and standing wave  $F_s$ . The probe locates the position where  $F_s = F_r$ . Using Equations (4), (8), equilibrium position of the probe is numerically analyzed as shown in Figure 6. Horizontal axis indicates the distance between the laser focus and the measured surface. Vertical

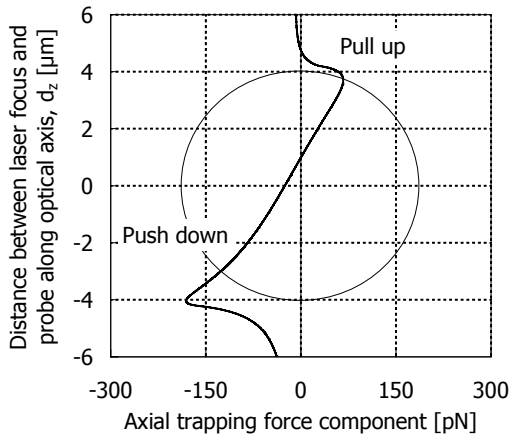


Fig. 5. The result of numerical analysis for axial trapping force during the laser focus deviates along the optical axis. Positive force, negative force is the force working upward and downward, respectively.

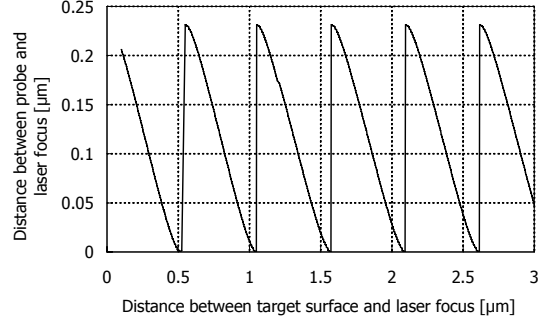


Fig. 6. Axial deviation of the probe from the laser focus with changing a distance between the sensor and a measured surface. This analytical result is calculated by using Equation (4), (8).

axis indicates the distance between the probe and the laser focus. When the probe is near to the laser focus,  $F_r$  is smaller than  $F_s$  due to the small  $d_z$ . As the measured surface moves, the probe begins to deviate from the laser focus, that is,  $F_r$  increases. When  $F_r$  grows over  $F_s$ , the probe abruptly changes the axial position from one stable point to another in the standing wave. Thus, the probe follows the saw-tooth wave liked pattern.

This sharp signal is used for detecting the standing wave pattern. In addition, the probe position between the peaks is considered almost linear. By interpolating the probe position between the peaks, fine motion of the measured surface is measurable. Thus, the distance between the laser focus and the measured surface is converted into the distance between the probe axial position and the laser focus.

## 4. EXPERIMENTAL SETUP

### 4.1 Optical system

Experimental apparatus is illustrated in Figure 7(a). This optical system is designed to compose the three elements: laser trapping, measurement of the probe motion and the imaging of the probe.

A laser diode excited fiber laser (Wavelength: 1064 nm, Polarization: linear, Max. laser power: 2.0 W) is employed for the trapping laser and also has the role to generate the standing wave. The trapping laser is focused by an objective lens (Olympus, NA0.95). For the probe, a glass micro-sphere ( $n=1.44$ ) of 8  $\mu\text{m}$  in diameter is used. A micro-sphere is optically trapped near the focus of the objective lens. A number of glass spheres are spread on the piezoelectric-actuator. Ultrasonic vibration of the piezoelectric-actuator induces the micro-sphere re-entrainment. Then the trapping laser successfully traps one of the particles. Laser diode (LD) (Wavelength: 640 nm, Laser power: 10 mW) is co-axially incident to the probe for measuring the probe axial motion. Backscattering light of the LD from the probe is collected by a photo-detector (PD). CCD camera takes the image of a trapped probe.

This optical system is accommodated as a compact unit [10]. The unit is carried by a precise 3-axes stage with positioning accuracy, which is better than 30 nm and full stroke 40 mm

### 4.2 Measurement system to measure probe position

The displacement due to the axial deflection of the probe is taken into account. As seen in Figure 6, the axial probe

motion is a few hundreds nanometers, so it is required to measure the probe deflection more precisely than 100 nm. Configuration of the detection system is shown in Figure 7(b) [11].

A PD is set on the optical axis. A collective lens converges a backscattered light from the probe,  $P_{total}$ . Illuminated area of the backscattered light,  $R_i$  is larger than effective area of the PD,  $R_d$ . Therefore, the average amount of the light that PD received,  $P_{ave}$  is expressed such as

$$P_{ave} = P_{total} (R_d / R_i)^2 \quad (9)$$

By assuming that the diffusion angle of backscattering light is constant,

$$R_i = (L - Z) \tan \theta \quad (10)$$

Then, the change of the detected power  $\Delta P_z$  is

$$\Delta P_z = \frac{dP_{ave}}{dz} \Delta z \cong \frac{2P_{ave} M_l}{L - Z} \Delta z \quad (11)$$

where,  $\Delta z$  is probe axial deflection and  $M_l$  is the longitudinal magnification. Thus, the probe axial deflection is linearly magnified according to Equation (9) into  $\Delta P_z$ . Magnification is varied by the power of the LD.

## 5. SCALE DETECTING PROPERTY

### 5.1 Accuracy of scale sensing

In order to examine the accuracy of the probe, the experiment was implemented that the probe approaches

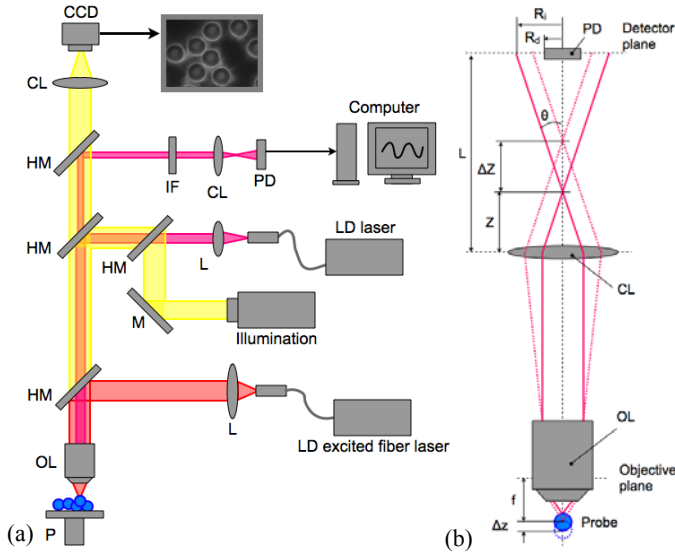


Fig. 7. (a) Optical system for a probe, which is derived from three elements: trapping a probe, measuring an axial motion of the trapped probe, imaging the trapped probe. The abbreviations are that L is lens, HM, half mirror, OL, objective lens, P, piezoelectric oscillator, M, mirror, CL, collective lens, IF, interference filter, PD, and photo detector. (b) Configuration of the detecting system for axial motion of the probe.  $R_i$ , illuminated area of the backscattered light,  $R_d$ , effective area of PD,  $f$ , focal length of the objective lens,  $\Delta z$ , probe axial deflection.

vertically to the measured surface at constant speed. In following fundamental experiments, a silicon wafer, which has smooth surface of better than 1 nm Ra is used.

Figure 8 shows the detected signals from the probe, when the probe is approaching toward the measured surface. The resultant signal is well agreed with the theoretical predicted signal shown in Figure 6. This proves that the probe is able to sense the interferometric scale.

Next, the detected pitch of the interferometric scale is analyzed. The wavelength of the trapping laser is 1064 nm, therefore the pitch of the interferometric scale should be 532 nm. Figure 9 is the histogram of detected pitch of the interferometric scale for sensing the scale at the distance of 100  $\mu\text{m}$ . The average pitch is 534 nm and the standard deviation is 16 nm. The error was 2 nm, in which the misalignment of the stage axis and optical axis of the probe are included.

### 5.2 Sensing resolution

The pitch of the scale is decided by the wavelength of the trapping laser, 532 nm in this case. The resolution, however, is derived from the probe sensitivity during interpolation. The resolution is examined by finding the distinguishable signal for certain displacement. Figure 10 shows the probe signal when the stage moves at intervals of 10 nm. Black line indicates raw data without any signal process. Red line is the data after processing through the low-pass filter. This probe is able to measure with the resolution better than 10 nm.

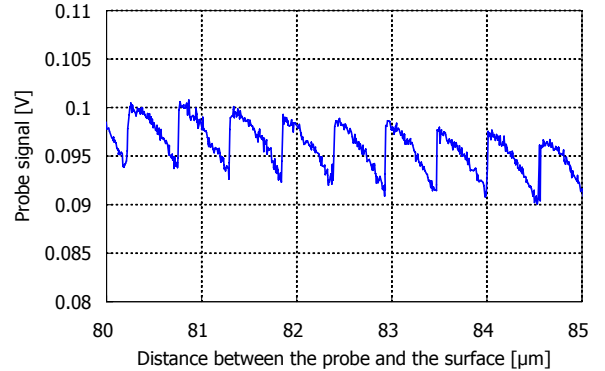


Fig. 8. Probe signal, which denotes the probe axial motion, when the probe approaches toward a measured surface.

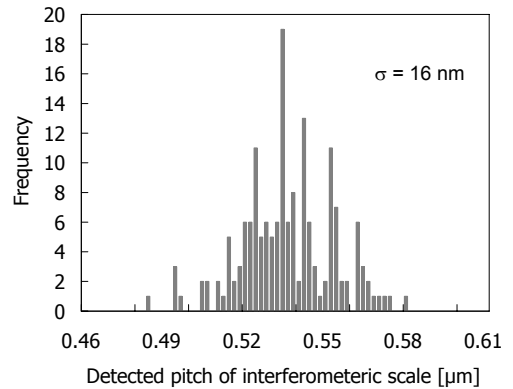


Fig. 9. Histogram of the detected pitches of the interferometric scale by the probe.

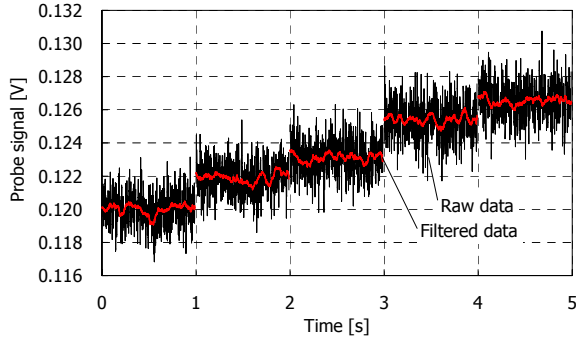


Fig. 10. Measuring resolution of the displacement sensor. The sensor signal when the measured surface moves at interval of 10 nm. Black and red line indicates raw data and data processed low pass filter, respectively.

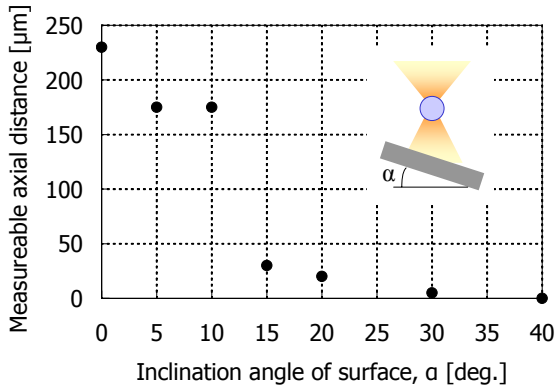


Fig. 11. Measurable distance of the interferometric scale.

### 5.3 Measurable inclination angle

Interference of the retro-reflected laser from the surface and the trapping laser generate the interferometric scale. Intensity of the retro-reflected light decreases by leaning the surface. Therefore, it is important to investigate the measurement property on the inclined surface. Especially at far from the surface, the forces by the interferometric scale decreases, so the measurable axial distance from the surface is chosen to evaluate the measurement property on the inclined surface. The measurable axial distance is determined by condition of whether the probe signal has saw tooth shape. The procedure is as follows. The sensing probe scans the surface laterally. The measurable axial distance from the surface is recorded when the abrupt probe signal is not identified. Only for non-tilted surface, the probe scans vertically. As the sample surface, the silicon wafer is used, which is leaned at certain angle.

The result is shown in Figure 11. On the inclination within  $10^\circ$ , a measurable axial distance is more than  $150 \mu\text{m}$ . For those more than  $15^\circ$ , the measurable axial distance suddenly becomes lower. According to the experiments, surface should not lean more than  $20^\circ$  for dimensional measurement. For large inclination, specular reflection does not perform to generate the interferometric scale.

### 5.4 Effective surface area for generating the scale

In order to evaluate the bottom surface, an optical probe must access the narrow area. In case of this technique, only paraxial component of the retro-reflected light generate the interferometric scale effectively. For trapping a microsphere

in air stably, a highly focused trapping laser is used. Therefore, the forward-scattering light beyond the probe may propagate at wide-angle. However, since the probe acts as collective lens, propagation of the forward-scattering light is narrower. For evaluating the lens effect of the microprobe, intensity of the paraxial forward scattered light is measured. The slit, which has a square aperture, is set 20 mm below the trapped probe align with optical axis. After the slit, a light intensity is measured. The structure of the measurement system is illustrated in Figure 12. The lens effect is evaluated as a parameter of certain scattered angular range that is calculated by the slit size. The results are summarized in Table 1. The result proves the performances of the lens effect by the trapped microsphere. The light intensity of paraxial scattered from the microsphere light becomes 1.6 times higher than those without the microsphere.

Then, it is confirmed that whether the paraxial retro-reflected light is able to generate the interferometric scale. The experiment is implemented that the probe signal is taken on the narrow beam. As the beam, the AFM cantilever is fabricated by a focused ion beam (FIB). The SEM image is shown in Figure 13. The width of the beam is  $15 \mu\text{m}$ . The

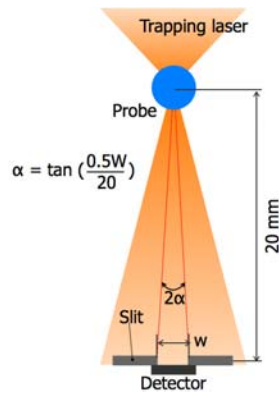


Figure 12. The angle of the forward-scattered light.

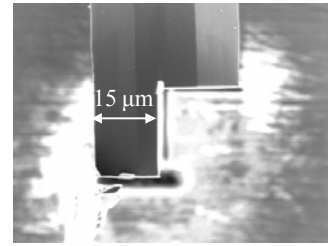


Figure 13. The specimen of the required surface is for generating the interferometric scale, which is a fabricated AFM cantilever beam by means of focused ion beam (FIB).

Table 1. Experimental results for lens effect of the trapped microsphere.

Scattered angle	Paraxial scattered light intensity	
	With probe	Without probe
$10.3^\circ$	55.9 mV	33.8 mV
$13.2^\circ$	107.4 mV	69.5 mV

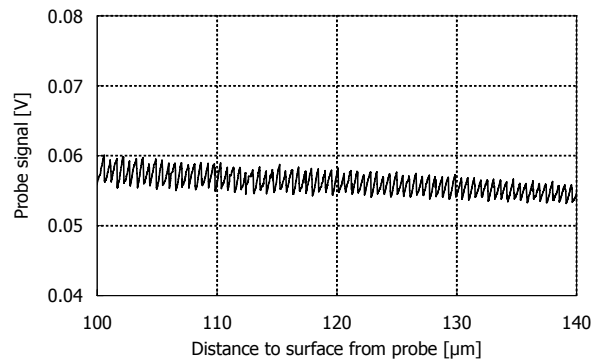


Figure 14. Probe signal on the narrow area of measured surface.



measured result is shown in Figure 14, which proves that the probe has sense the useful signal even at axial distance of more than 100  $\mu\text{m}$  on the surface. This implies that the proposed technique can access the narrow area of the surface.

## 6. MEASUREMENT OF 3D SHAPE

Finally, to investigate the ability of dimensional measurement by the proposed technique, one of the cross-sectional shape of a silicon sphere is measured. A nominal diameter of the silicon sphere is 1 mm. The probe scans several dozen  $\mu\text{m}$  above the top surface of the sphere in a straight line over 250  $\mu\text{m}$ . The measured data is shown in Figure 15. Circular fitting is implemented and the error between fitting and measured data is also plotted.

It is confirmed that the top surface surrounding the sphere can be measured by using this technique. The error from fitting curve is approximately 100 nm in 100  $\mu\text{m}$  from the center, which is equivalent to the surface inclination angle of  $11.5^\circ$ . In the area of outer than 100  $\mu\text{m}$ , the error becomes larger because the inclination of surface increases more than  $15^\circ$ . As implied in section 5.3, this technique is effective at the surface inclined up to  $15^\circ$ . In this time, the measurement data is taken while detecting fiducial points of interferometric scale. By interpolation of the data, continuing data is obtained. In terms of the measurement accuracy, it is around 100 nm in this experiment.

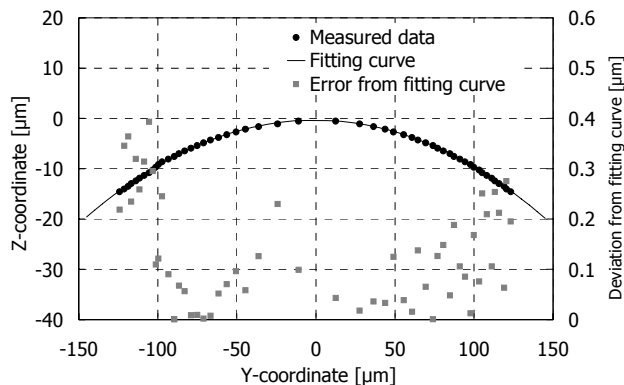


Fig.15. Dimensional measurement of one cross-section of a silicon sphere.

## 7. CONCLUSION

It is proposed that the new dimensional measurement technique using the laser-trapped micro-sphere as the sensing probe and the interferometric scale as the length scale. This technique aims to measure bottom surface of the shape such as fresnel lens and grooves.

In this paper, as fundamental study, principle of the measurement is confirmed by considering the optical trapping forces and the forces by the interferometric scale. This principle is experimentally confirmed that the sensor probe performs to read the interferometric scale with the accuracy of  $\pm 16 \text{ nm}$  ( $1\sigma$ ). Resolution of this measurement technique is estimated as 10 nm. The optically trapped microsphere acts as collective lens, so that the laser intensity of the paraxial rays is enhanced. As the result, paraxial

scattering light is able to compose the interferometric scale. Therefore, this technique makes it possible to access the narrow area. The measurable range of the inclination angle of surface is less than  $15^\circ$ , which is confirmed both fundamental experiment and dimensional measurement of the sphere. In terms of the measurement accuracy, it is estimated as 100 nm from the dimensional measurement of the top surface of the silicon sphere. To improve the accuracy, following points must be dedicated in future. The first one is to improve the pitch of the interferometric scale. The pitch of the interferometric scale is half of the trapping laser. So, as light source for trapping laser, the laser having shorter wavelength should be employed. The second one is to improve the measurement of the axial displacement of the sensing probe. As estimated in section 3.3, the sensing probe deviates several 100 nm. Therefore, at least 1  $\mu\text{m}$  range is required to be measurable. However, it is not easy to obtain a linear signal against probe motion over 1  $\mu\text{m}$ . Accurate measurement of axial displacement of the probe leads more accurate dimensional measurement.

## ACKNOWLEDGEMENTS

This study is partly supported by a Grant-in-Aid for JSPS (Japanese society for the promotion of science) Fellows.

## REFERENCES

- [1] H.N. Hansen, K. Carneiro, H. Haitjema, and L. De Chiffre, "Dimensional Micro and Nano Metrology", *Annals of the CIRP*, vol.55(2), pp. 721-743, 2006.
- [2] A. Weckenmann, P. Kraemer and J. Hoffmann, "Manufacturing metrology –State of art and prospects", *Proc. ISMQC*, pp. 1-8, Madras, India, Nov. 2007.
- [3] H. Tsutsumi, K. Yoshizumi, and H. Takeuch, "Ultrahigh Accurate 3-D Profilometer", *Proc.SPIE*, vol.5638, pp. 387-394, 2005.
- [4] S.C.H. Thian, W. Feng, J.Y.H. Fuh, H.T. Loh, K.H. Tee, Y. Tang, and L. Lu, "Dimensional measurement of 3D microstructure based on white light interferometer", *J. Phys: Conf. Series*, vol.48, pp. 1435-1446, 2006.
- [5] E.J.C. Bos, F.L.M. Delbressine, H. Haitjema, "High-accuracy CMM metrology for micro systems", *Proc. ISMQC*, pp. 511-522, Erlangen, Germany, Oct. 2004.
- [6] A. Ashkin, J.M. Dziedzic, J.E. Bjorkholm, and S. Chu, "Observation of a single-beam gradient force optical trap for dielectric particles", *Opt. Lett.*, vol.11, pp. 288-290, 1986.
- [7] M. Michihata, Y. Takaya, and T. Hayashi, "Nano position sensing based on laser trapping technique for flat surfaces" *Meas. Sci. Technol.* vol.19, pp. 084013, 2008.
- [8] A. Ashkin, "Forces of a single-beam gradient laser trap on a dielectric sphere in the ray optics regime," *Biophys. J.*, vol.61, pp. 596-582, 1992.
- [9] W. Mu, Z. Li, L. Luan, G.C. Spalding, G. Wang, and J.B. Ketterson, "Force measurement on microspheres in an optical standing wave", *J. Opt. Soc. Am. B*, vol.25, pp. 763-767, 2008.
- [10] M. Michihata, Y. Takaya and T. Hayashi, "Development of the nano-probe system based on the laser trapping technique" *Annals of the CIRP*, vol.57(1), pp. 493-496, 2006.
- [11] M.E.J. Friese, A.G. Truscott, H. Rubinsztein-Dunlop, and N. R. Heckenberg, "Determination of the force constant of a single-beam gradient trap by measurement of backscattered light" *Appl. Opt.*, vol.35, pp. 7112-7116, 1996.